Acta of Bioengineering and Biomechanics
Vol. 15, No. 1, 2013

Original paper
DOI: 10.5277/abb130102

In vivo study of human mandibular distraction osteogenesis. Part II: Determination of callus mechanical properties

ANNE-SOPHIE BONNET[1], GUILLAUME DUBOIS[2], PAUL LIPINSKI[1]*, THOMAS SCHOUMAN[3]

[1] Laboratory of Mechanics, Biomechanics, Polymers and Structures, Ecole Nationale d'Ingénieurs de Metz, Metz Cedex, France.
[2] Orthopédie Biomécanique Locomotion, Chatillon, France.
[3] AP-HP, Department of Maxillo-facial Surgery, Pitié-Salpétrière University Hospital, Faculty of Medicine, Paris, France.

Distraction Osteogenesis (DO) is a surgical technique used to reconstruct bone defects. To improve the current treatment protocols, the knowledge of the mechanical properties of the bone regenerate is of major interest. The aim of this study, constituting the second part of our paper previously published in Acta of Bioengineering and Biomechanics, was to identify the elastic and viscous properties of bone callus. This is done in the case of a mandibular DO by analyzing the experimental measurements of the forces imposed on bone regenerate by a distraction device. The bone transport forces were evaluated thanks to strain gauges glued on the distraction device. A rheological model describing the callus constitutive behavior was developed and the material constants involved were identified. The time-dependent character of the bone regenerate mechanical behavior was confirmed. The viscous response of the mesenchymal tissue was described by two characteristic times. The first one describing the viscoelastic callus behavior was estimated to be 140 seconds and the second one representing the permanent bone callus lengthening was evaluated to be 5646 seconds. An average value of 0.35 MPa for the regenerate Young's modulus was deduced. The elastic properties of mesenchymal tissue found are in agreement with the rare data available in the literature.

Key words: *mandibular distraction osteogenesis, rheological model, callus mechanical properties*

1. Introduction

Distraction osteogenesis (DO) is a biological tissue reconstruction process adopted to lengthen limb bones or to correct severe bone defects. During the surgical act, a gap is created between two bone segments which is rapidly fulfilled by mesenchymal tissue. The distraction protocol consists in applying daily a displacement on the gap tissue through an internal or external mechanical device. The mechanical loading imposed on the regenerated tissue directly influences the cells differentiation (Ilizarov [1]). Consequently, the parameters of the distraction protocol have to be carefully chosen in order to produce bone tissue of good quality (Richards et al. [2], Boccaccio and Kelly [3]). Among those parameters, the distraction rate, distraction frequency, distractor stiffness, latency duration have been identified to play a significant role on the clinical issue (Ilizarov [4], [5], Li et al. [6], al Ruhaimi [7], King et al. [8], Reina-Romo et al. [9]). The influence of these parameters has often been studied through computational models (Idelsohn et al. [10], Loboa et al. [11], Samchukov et al. [12]). The reliability of the numerical simulations is strongly dependent on the mechanical properties of the regenerated tissue introduced into the model. However, the measurement of these mechanical properties is very delicate and only a few authors have addressed this topic.

The time-dependent character of bone regenerate behavior was observed in several studies concerning among others the distraction of the lower limbs in animals (Aronson and Harp [13]; Brunner et al. [14])

* Corresponding author: Paul Lipinski, Laboratory of Mechanics, Biomechanics, Polymers and Structures, Ecole Nationale d'Ingénieurs de Metz, 1 route d'Ars Laquenexy CS 65820, 57078 Metz Cedex, France. Tel: 33 3 87 34 42 63, fax: 33 3 87 34 69 35, e-mail: lipinski@enim.fr

Received: March 26th, 2012
Accepted for publication: September 28th, 2012

and humans (Gardner et al. [15]; Gardner et al. [16]; Wolfson et al. [17]; Younger et al. [18]). An *in vitro* study (Richards et al. [2]) proposed an approach to characterize viscoelastic constitutive law of the bone callus. Leong and Morgan [19] evaluated the elastic properties of bone callus on rats using nanoindentation techniques.

Some authors tried to deduce this property. Lacroix et al. [20] determined a value for Young's modulus of callus from tension tests. Reina-Romo et al. [9] suggested a general expression allowing Young's modulus of the granular tissue to be determined in function of its composition.

It is proposed in the present work to characterize the mechanical properties of bone regenerate during the early phases of human mandibular DO from the measurement of bone transport forces and callus elongation.

2. Methods

2.1. Context

The case of a 37-year-old male undergoing a mandibular reconstruction by osteogenic distraction was considered. The external device (DEOS, OBL, France) illustrated in Fig. 1a was used. A distraction rate of 1 mm/day at a frequency of twice a day was adopted in agreement with classical distraction protocols. Thanks to strain measurements by gauges glued on some of the distractor pins (see Fig. 1b), distraction forces and callus elongation during the first week of treatment could be determined. A six strain record database of variable duration t_{end} (see Table 1) was built. A complete experimental procedure and mechanical analysis leading to these forces is detailed in the first part of this work [21].

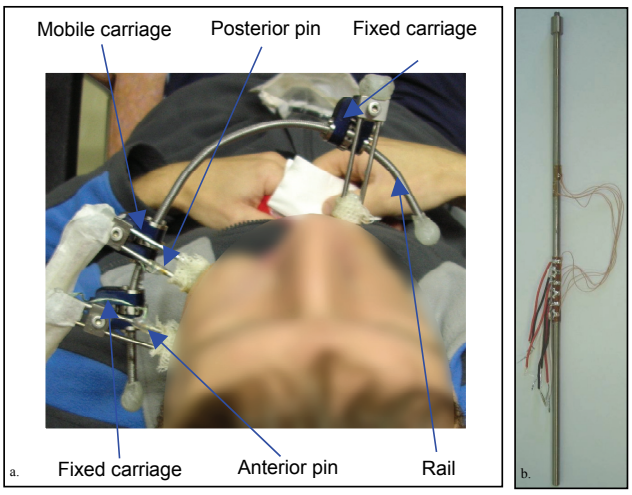

Fig. 1. Views of the whole custom made bone transport device (a) and pin equipped with strain gauges (b)

Table 1. Record duration

Activation number	1	2	3	4	5	7
t_{end} [s]	93	400	5400	1130	1100	4400

The aim of this paper was to propose a rheological model allowing the elastic and viscous properties of the callus to be determined by comparing the predictions of this model with the experimental force versus time curves.

2.2. Rheological model

It was found in our previous work [21] that the distraction force versus time curves all displayed the same trend represented by three distinct phases. A typical curve corresponding to the average signal obtained during the seventh activation is reported in Fig. 2.

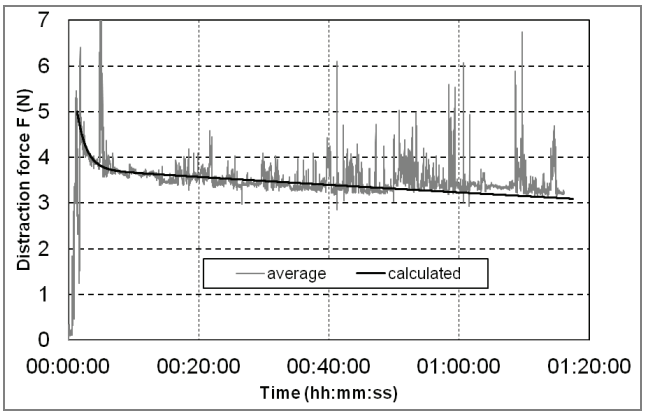

Fig. 2. Comparison between experimental and model predicted distraction force for the 7th activation

The first phase of strong increase of the distraction force was identified to be mainly linked to the elastic deformation of the distractor pins. Therefore, the first rheological element introduced in our model was a spring with stiffness K corresponding to the DEOS flexibility.

The exponential decrease of the distraction force observed in the second phase was attributed to the callus viscoelastic relaxation process represented by a relaxation time τ_e. To reproduce this viscoelastic behavior, a parallel assembly of a dashpot with viscosity μ_e and a spring having stiffness k was considered (Kelvin's model).

In the third phase, a second viscous mechanism of characteristic time $\tau_{vp} \gg \tau_e$ was pointed out, as a continuous decrease of the distraction force in a nearly linear manner was observed. The viscoplastic behavior of the bone regenerate was supposed to be responsible for this latter stage. This permanent viscous behavior is described in our rheological model through the parallel assembly of a dashpot with viscosity μ_{vp} and a slider characterized by its threshold force F_T.

As an additive decomposition of the total callus strain into elastic and permanent parts is supposed in this work, the viscoelastic and viscoplastic branches of the rheological model were assembled in series. A complete rheological scheme considered is illustrated in Fig. 3.

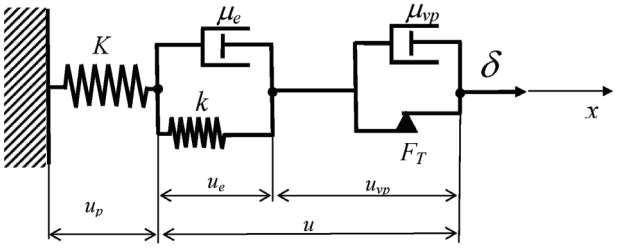

Fig. 3. Rheological model of the callus behavior

2.3. Estimating mechanical properties of callus

The constitutive laws of rheological elements involved in this model are summarized below

$$\begin{aligned} F_p &= Ku_p, \\ F_e &= ku_e, \\ F_v &= \mu_e \dot{\mu}_e, \\ F_{vp} &= \mu_{vp} \dot{\mu}_{vp}. \end{aligned} \tag{1}$$

In these expressions, u_e and u_{vp} represent the elongation of the viscoelastic and viscoplastic branches of the rheological model, respectively. The displacement of the distractor pin is denoted by u_p. The derivation with respect to time is marked by a dot over the variable considered. For example, $\dot{u}_e$ indicates the elongation velocity of the viscoelastic branch. The forces acting in the rheological parts are indicated by capital letter F with corresponding subscripts. K and k denote the stiffness of the distractor pins and that of the spring of Kelvin's model, respectively.

To determine the differential equation of the model, equilibrium and compatibility equations have to be considered. They take the form

$$F_p = F_{ve} = F_e + F_v = F_{vp} + F_T = F, \tag{2}$$

$$\delta = u_p + u_e + u_{vp}, \tag{3}$$

where δ is the total displacement of the distraction device and callus. The slider threshold force F_T could not be precisely determined from the experimental results described in [21] as all records performed were relatively short in time (see Table 1). However, as was mentioned in our previous paper [21], all the values of the recorded strains had returned to zero before the beginning of new activation. This indicated that a complete unloading of the distraction device had occurred after a twelve-hour period. Consequently, the slider threshold force F_T was assumed to be nil in the following developments.

Thus, combining expressions (1) and (3) and neglecting F_T, the differential equation for the permanent viscous dashpot displacement could be obtained

$$\frac{d^2 u_{vp}}{dt^2} + a_1 \frac{du_{vp}}{dt} + a_2 u_{vp} = a_2 \delta, \tag{4}$$

with

$$\begin{aligned} a_1 &= \frac{\mu_{vp}(k+K) + K\mu_e}{\mu_{vp}\mu_e}, \\ a_2 &= \frac{Kk}{\mu_{vp}\mu_e}. \end{aligned} \tag{5}$$

This differential equation can be solved using the following initial conditions

$$u(0) = 0,$$

$$u_p(0) = \delta \;\rightarrow\; F(0) = k\delta.$$

The solution of (4) can be written as

$$\mu_{vp}(t) = \frac{\delta}{\mu_{vp}(r_2 - r_1)} \left[\mu_{vp}(r_2 - r_1) - (K + r_2\mu_{vp})\exp(r_1 t) + (K + r_1\mu_{vp})\exp(r_2 t)\right] \tag{6}$$

where

$$r_{1,2} = -\frac{(k+K)\mu_{vp} + K\mu_e}{2\mu_{vp}\mu_e} \pm \sqrt{\left(\frac{(k+K)\mu_{vp} + K\mu_e}{2\mu_{vp}\mu_e}\right)^2 - \frac{Kk}{\mu_{vp}\mu_e}}. \quad (7)$$

Knowing this permanent viscous displacement, the expression of the distraction force can be obtained using (1_4) and (2)

$$F(t) = \frac{\delta}{(r_2 - r_1)} [(K + r_1\mu_{vp})r_2 \exp(r_2 t) - (K + r_2\mu_{vp})r_1 \exp(r_1 t)]. \quad (8)$$

The fitting of the experimental distraction force versus time curves enables the rheological constants μ_e, k and μ_{vp} to be identified. To deduce the mechanical properties of callus, the usual expressions are used

$$E_c = \frac{kl_c}{A_c},$$

$$\eta_e = \frac{\mu_e l_c}{A_c},$$

$$\eta_{vp} = \frac{\mu_{vp} l_c}{A_c},$$

where E_c, η_e, and η_{vp} are Young's modulus of the callus and elastic and permanent viscosities, respectively. In these expressions, A_c and l_c stand for the current cross-section area and length of regenerate.

3. Results

The six curves of distraction force versus time were fitted with expression (8) to identify mechanical properties of the callus. Among all rheological parameters involved in this equation, the DEOS stiffness can be determined as a function of its dimensions using the following expression

$$K = \frac{12EI}{l_F^3 + l_M^3} \frac{8I + 2a^2 A}{16I + a^2 A} = \frac{390EI}{17(l_F^3 + l_M^3)} \approx 9 \frac{\text{N}}{\text{mm}},$$

with l_F and l_M corresponding to the length of the fixed carriage pin and the mobile carriage pin, respectively. The values of the parameters and the signification of the remaining ones are provided in our previous paper [21].

This value is in good agreement with the one of 10.03 N/mm estimated experimentally in [21].

All other rheological parameters are obtained by the fitting procedure. Figure 2 illustrates the best fit for activation 7. Table 2 summarizes the rheological parameters and the associated material constants for all activations analyzed. The tissue properties have been obtained under approximation of a constant regenerate cross section area A_c = 285 mm^2. The last row of Table 2 indicates the model prediction of the distraction force F_{12h} after twelve hours of lengthening (period between two successive activations).

Table 2. Rheological and material parameters

Activation	1	2	3	4	5	7
l_c (mm)	1.5	2	2.5	3	3.5	4.5
k (N/mm)	20	20	30	35	35	35
μ_e (Ns/mm)	3000	4000	4000	5000	3665	3610
μ_{vp} (Ns/mm)	2000	100000	150000	200000	230000	180000
E (MPa)	0.14	0.14	0.26	0.37	0.43	0.55
η_e (MPas)	21	28	35	53	45	57
η_{vp} (MPas)	14	702	1316	2105	2824	2842
F_{12h} (N)	0	0.2	0.54	0.74	0.4	0.62

The values of rheological parameters and mechanical constants of the callus are consistent with one another. The stiffness of the callus is rising with the activation number (distraction time), leading to a significant increase of Young's modulus from 0.14 to 0.55 MPa. The evolution of the elastic viscosity follows the same trend as the value of η_e grows from 21 to 57 MPas. Since the durations of records 1 and 2 are very short (see Table 1), precise estimation of the callus permanent viscous properties was impossible for these two activations. Consequently, the corresponding values in Table 2 are grayed and will not be taken into account in the discussion (Section 4). However, the four exploitable values of η_{vp} also indicate a tendency for the callus to increase this viscosity as a function of time. For all activations, the model predicted values of the distraction force after a period of 12 hours, corresponding to the time interval between two successive activations, are close to zero.

4. Discussion

4.1. Plastic threshold

The precise identification of the threshold force of the dashpot can only be achieved from long time rec-

ords and especially from the value of residual force at the end of each lengthening cycle. In our work, precise determination of this residual force F_{12h} after 12 hours of lengthening was not possible because of the drift of the electronic signals observed. Consequently, it was supposed, see Section 2, that the slider threshold force F_T was equal to zero. This choice is motivated by the previous works of Labbé et al. [22] using DEOS. The authors observed that the desired bone lengthening always corresponded to a scheduled number of activations with a constant increment of displacement. This indicates that at the end of each lengthening cycle, the regenerate elongation magnitude is close to the imposed incremental displacement. In our model, the predicted residual force varies between 0.4 and 0.74 N, values which are ten times smaller than the recorded peak forces. The regenerate lengthening associated to these forces ranges from 0.42 to 0.46 mm. This suggests that the assumption of a zero threshold force in our model is adequate.

4.2. Relaxation times

The values of the mesenchymal tissue properties obtained by the model permit the characteristic times of both deformation mechanisms to be determined. They are defined by the following expressions

$$\tau_e = \frac{\mu_e}{k} = \frac{\eta_e}{E},$$

$$\tau_{vp} = \frac{\mu_{vp}}{k} = \frac{\eta_{vp}}{E}.$$

Table 3 gives these characteristic times for the six records corresponding to the valid tests.

The viscoelastic relaxation time varies between 104 and 200 seconds. Its average value was estimated to be τ_e = 140 s. Except activation 2, the tendency of slow decrease of this property as a function of time can be noticed. This decrease indicates the probable evolution of the callus, during four days of measurements, towards a more elastic constitution. For four sufficiently long records, the permanent viscous characteristic time has been estimated. This property changes between 5167 and 6567 seconds leading to the average value of τ_{vp} = 5646 s. The important ratio between τ_{vp} and τ_e (about 40) emphasizes the existence of two well distinguishable viscous deformation modes justifying the constitutive modeling proposed.

The analysis performed by Richards et al. [2] provided also two viscous nonlinear deformation modes characterized by a cubic relaxation function such that

$$G(\varepsilon(t),t) = [g_{1\infty} + g_{11}e^{-t/\tau_{11}} + g_{12}e^{-t/\tau_{12}}]\varepsilon$$

$$[g_{3\infty} + g_{31}e^{-t/\tau_{31}} + g_{32}e^{-t/\tau_{32}}]\varepsilon^3$$

where ε is a strain measure not specified by the authors. In the sequel, it is supposed that this measure corresponds to Hencky's logarithmic strain.

The material constants involved in the expression of relaxation function were determined by the *in vitro* short time relaxation tests on six rabbit tibiae. All these tibiae were lengthened 9 mm during twelve-day distractions. The average relaxation times identified by these tests were: $\tau_{11} \approx \tau_{31} \approx 12$ and $\tau_{12} \approx \tau_{32} \approx 150$ seconds. Another important property of the rabbit mesenchymal tissue can be deduced from the work of Richards et al. [2]. They remarked that "yielding and/or damage was apparent" in four of the six test specimens submitted to "the 1000 μm step" displacement. This remark enables the critical strain of 18 day-old rabbit callus to be estimated. Using the logarithmic strain definition one gets $\varepsilon_D = \ln\left(\frac{10.0}{9.0}\right) = 0.10.$

A comparison of these characteristics with our results leads to the following remarks:

- The loading or activation time in our experiments was relatively long (about 10 to 60 seconds). Consequently, the relaxation time of about 10 seconds observed by Richards et al. [2] cannot be identified from the records presented in this work.
- The second relaxation time determined by Richards et al. [2] is in very good agreement with the viscoelastic characteristic time τ_e deduced from our tests.
- On the other hand, the relaxation tests reported in [2] were too short (100 seconds) to access the second characteristic time τ_{vp} identified in our work. Besides, the *in vitro* conditions of Richards' tests also exclude the possibility of its identification; see additional comments on this subject below.

Table 3. Characteristic times of regenerate viscous deformation mechanisms

Activation	1	2	3	4	5	7	Average
τ_e [s]	150	200	135	143	105	104	140
τ_{vp} [s]	–	–	5161	5689	6567	5167	5646

Based on their relaxation times, Richards et al. [2] performed numerical simulations to estimate the tension (force) accumulation during the successive incremental loading of mesenchymal tissue from l_o = 2.25 mm to l_f = 9.0 mm. Amongst other results, they found that after a seven-day lengthening period of the rabbit tibia callus, the accumulated tension stress tended towards an asymptotic value of 2.5 MPa for two distraction rates of 0.250 mm four times daily and 0.5 mm twice daily. According to Richards et al. [2], this tension stress corresponds to a residual or accumulated force of about 100 N. Such a high value is in disagreement with our experimental observations and numerical predictions. We recall that our model leads to $F_{12h} \approx 0.5$ N. Two major points render the conclusions of Richards et al. [2] uncertain. First, as depicted by their figure 9, the slow relaxation process is monitored during the whole cycle time of 6 or 12 hours, after each activation. However, with the characteristic times of 12 and 140 seconds announced in their paper, the relaxation process should be practically achieved after 0.5 h as the value of the exponential kernel corresponding to the longest relaxation time of 140 s becomes negligible ($\exp(-1800/140) = 2.6 \cdot 10^{-6}$). Consequently, all curves corresponding to the various distraction strategies with the same daily distraction rate have to be superimposed, except for the short duration peaks subsequent to new activation. Furthermore, the predicted accumulated tension stress level seems also inaccurate. To estimate this stress, the mesenchymal tissue properties can be extracted from figures 6 and 8 of [2]. These data, corresponding to test 2, are: $g_{1\infty} = 0.3$, $g_{11} = 0.174$, $g_{12} = 0.155$, $g_{3\infty} = 185$, $g_{31} = 16.37$ and $g_{32} = 97.69$. All these moduli are expressed in MPa. The strain measure definition to be used in such calculations is also of major importance as the final simulated stretch of the mesenchymal tissue is rather important; $\lambda_f = 9/2.25 = 4$.

Let us consider the case of the distraction rate of 0.5 mm twice daily. The strain step for first increment is $\varepsilon_1 = \ln\left(\frac{2.75}{2.25}\right) = 0.20$ and the final callus strain becomes $\varepsilon_f = \ln(\lambda_f) = 1.39$. To verify the consistency of the data identified, let us first calculate the tension level at $t = 0$, i.e., immediately after the first activation. In this case, the relaxation function leads to $\sigma(0) = (g_{1\infty} + g_{11} + g_{12})\varepsilon_1 + (g_{3\infty} + g_{31} + g_{32})(\varepsilon_1)^3 = 2.52$ MPa. This value is in very good accordance with figure 9 from [23]. To determine the stress value at the end of the k-th cycle the following formula can be used

$$\sigma_k = g_{1\infty}\sum_{i=1}^{k}\varepsilon_i + g_{3\infty}\left(\sum_{i=1}^{k}\varepsilon_i\right)^3,$$

since, as demonstrated above, the quasi-full stress relaxation is obtained after 0.5 hour. When applied to cycle 1 it leads to: $\sigma_1 = g_{1\infty}\varepsilon_1 + g_{3\infty}(\varepsilon_1)^3 = 1.54$ MPa. This value is much lower but still comparable with the result presented in [23] (2.1 MPa). At the end of distraction process, one gets $\sigma_f = g_{1\infty}\varepsilon_f + g_{3\infty}(\varepsilon_f)^3 = 508.0$ MPa which is 200 times greater than ≈ 2.5 MPa obtained in [2]. Moreover, the damage strain $\varepsilon_D = 0.10$ deduced above for freshly distracted mesenchymal tissue enables its mechanical strength to be estimated; $\sigma_D \le (g_{1\infty} + g_{11} + g_{12})\varepsilon_D + (g_{3\infty} + g_{31} + g_{32})(\varepsilon_D)^3 = 0.36$ MPa. Consequently, callus fracture should occur for stresses larger than this value and should produce the full relaxation of accumulated tensions. These incompatible results prove that the viscoelastic constitutive law proposed by Richards et al. [2] is insufficient to describe the mesenchymal tissue behavior during callus lengthening. As was demonstrated by Wolfson et al. [17] the predistractional resting or residual forces evolve differently *in vitro* and *in vivo*. For large lengthening of human lower limb, *in vitro* forces were 2.7 times greater than *in vivo* experiments. The authors attributed this residual traction to the forces exerted in soft tissues or to muscular activity. In our case of mandible with multi-tissular facial defect from a gunshot trauma, the resistance of these soft tissues can be probably neglected and was ignored in our study.

Gardner et al. [16] introduced the notions of viscoelastic recoverable and long term non-recoverable extensions of biological biphasic tissues. In lengthening processes, they attributed the peak force to the first viscoelastic deformation mode due to the immediate response of the tissue with "trapped" liquid phase inside. The non-recoverable deformation mode, with a long relaxation time, is accredited to the fluid phase transfer between zones with different fluid pressures. Also, the morphological and volumetric changes of constituents and their properties are included in this irreversible deformation mode. This description corresponds to the experimental results obtained in our study. The second characteristic time of about 5650 seconds, found in our work and determined from four sufficiently long records, characterizes the mean rate of this permanent lengthening of regenerate. However, the rheological model of Maxwell fluid proposed in our study, eventually nonlinear with a threshold force evolving in function of callus constitution, seems to be adapted for describing the regenerate lengthening, at least in one dimensional configuration.

4.3. Elastic properties of regenerate

To estimate the regenerate elastic properties, a rough hypothesis concerning its cross section area was adopted. It was supposed that this last one corresponds to the osteotomy cross section area determined by the pre-distraction CT scan exam, and did not evolve during the distraction. As indicated in Table 2, Young's modulus of the callus deduced from the records increased in function of the post-operative day from 0.14 MPa for the first activation (post-operative day 7) to 0.55 MPa for the seventh activation (post-operative day 11). Such a rapid evolution of elastic properties in human is certainly exaggerated. At least partially, it can be attributed to the constant cross section area hypothesis as well as to the "manual" fitting procedure used to reproduce the experimental force versus time records. However, the average value of $E = 0.35$ MPa is consistent with the rare data from the literature concerning the properties of the mesenchymal tissue during the early stage of distraction. For instance, the results of Richards et al. [2] provide the value of the secant Young's modulus of regenerate E_S as a function of the applied strain (nonlinear elasticity) $E_S = g_{1\infty} + g_{3\infty}\varepsilon^2$. In the case of small strains ($\varepsilon \leq 0.05$), and using the data from figures 6 and 8 of [2], this expression provides $0.3 \leq E_S \leq 0.76$ MPa, which is in excellent agreement with our measurements.

In a recent work of Leong and Morgan [19], where nanoindentation techniques were used to identify the elastic properties of the rat granular tissue, the average value of Young's modulus found was 0.99 MPa. The tests were undertaken at post fracture day 35. As expected, this value is higher than our maximal result obtained at post-operative day 11 in human.

Lacroix et al. [20] obtained a value of 0.2 MPa for Young's modulus when submitting a 3 mm callus gap to a tension force of 500 N.

Reina-Romo et al. [9] calculated a value of approximately 5 MPa for the same elastic property by using their general expression of Young's modulus in function of its composition. However, in the more recent work of Reina-Romo [24] the value of Young's modulus was reconsidered and taken to be equal to 1 MPa in reference to the work of Leong and Morgan [19].

This comparative analysis seems to confirm the capacity of the callus constitutive model proposed in this work to identify the viscoelastic and permanent properties of bone regenerate during distraction osteogenesis using DEOS.

References

[1] ILIZAROV G.A., *The Tension-Stress Effect on the Genesis and Growth of Tissues. Part II. The Influence of the Rate and Frequency of Distraction*, Clin. Orthop. Relat. Res., 1989b, 239, 263–285.

[2] RICHARDS M., WINEMAN A.S., ALSBERG E., GOULET J.A., GOLDSTEIN S.A., *Viscoelastic characterization of mesenchymal gap tissue and consequences for tension accumulation during distraction*, ASME J. Biomech. Eng., 1999, 121, 116–123.

[3] BOCCACCIO A., PAPPALETTERE C., KELLY D.J., *The Influence of Expansion Rates on Mandibular Distraction Osteogenesis: A Computational Analysis*, Ann. Biomed. Eng., 2007, 35, 1940–1960.

[4] ILIZAROV G.A., *The principles of the Ilizarov method*, Bull. Hosp. Jt Dis. Orthop. Inst., 1988, 48, 1–11.

[5] ILIZAROV G.A., *The Tension-Stress Effect on the Genesis and Growth of Tissues. Part I. The Influence of stability of fixation and soft-tissue preservation*, Clin. Orthop. Relat. Res., 1989a, 238, 249–281.

[6] LI G., SIMPSON H.R.W., KENWRIGHT J., TRIFFITT J.T., *Tissues formed during distraction osteogenesis in the rabbit are determined by the distraction rate: localization of the cells that express the MRNAS and the distribution of types I and II collagens*, Cell. Biol. Int., 2000, 24, 24–33.

[7] al RUHAIMI K.A., *Comparison of different distraction rates in the mandible: an experimental investigation*, Int. J. Oral Maxillofac. Surg., 2001, 30, 220–227.

[8] KING N.S., LIU Z.J., WANG L.L., CHIU I.Y., WHELAN M.F., HUANG G.J., *Effect of distraction rate and consolidation period on bone density following mandibular osteodistraction in rats*, Arch. Oral Biol., 2003, 48, 299–308.

[9] REINA-ROMO E., GÓMEZ-BENITO M.J., GARCÍA-AZNAR J.M., DOMÍNGUEZ J., DOBLARÉ M., *Modeling distraction osteogenesis: analysis of the distraction rate*, Biomech. Model. Mechanobiol., 2009, 8, 323–335.

[10] IDELSOHN S., PLANELL J.A., GIL F.J., LACROIX D., *Development of a dynamic mechano-regulation model based on shear strain and fluid flow to optimize distraction osteogenesis*, J. Biomech., 2006, 39, S9–S10.

[11] LOBOA E.G., FANG T.D., PARKER D.W., WARREN S.M., FONG K.D., LONGAKER M.T., CARTER D.R., *Mechanobiology of mandibular distraction osteogenesis: finite element analyses with a rat model*, J. Orthop. Res., 2005, 23, 663–670.

[12] SAMCHUKOV M.L., COPE J.B., HARPER R.P., ROSS J.D., *Biomechanical considerations of mandibular lengthening and widening by gradual distraction using a computer model*, J. Oral Maxillofac. Surg., 1998, 56, 51–59.

[13] ARONSON J., HARP J.H., *Mechanical forces as predictors of healing during tibial lengthening by distraction osteogenesis*, Clin. Orthop. Relat. Res., 1994, 301, 73–79.

[14] BRUNNER U.H., CORDEY J., SCHWEIBERER L., PERREN S.M., *Force required for bone segment transport in the treatment of large bone defects using medullary nail fixation*, Clin. Orthop. Relat. Res., 1994, 301, 147–155.

[15] GARDNER T.N., EVANS M., SIMPSON A.H., KENWRIGHT J., *A method of examining the magnitude and origin of soft and hard tissue forces resisting limb-lengthening*, J. Biomed. Eng., 1997, 19, 405–411.

[16] GARDNER T.N., EVANS M., SIMPSON H., KENWRIGHT J., *Force-displacement behaviour of biological tissue during*

distraction osteogenesis, Med. Eng. Phys., 1998, 20, 708–715.

[17] WOLFSON N., HEARN T.C., THOMASON J.J., ARMSTRONG P.F., *Force and stiffness changes during Ilizarov leg lengthening*, Clin. Orthop. Relat. Res., 1990, 250, 58–60.

[18] YOUNGER A.S.E., MACKENSIE W.G., MORRISON J.B., *Femoral forces during limb lengthening in children*, Clin. Orthop. Relat. Res., 1994, 301, 55–63.

[19] LEONG P.L., MORGAN E.F., *Measurement of fracture callus material properties via nanoindentation*, Acta Biomater., 2008, 4, 1569–1575.

[20] LACROIX D., PRENDERGAST P.J., *A mechano-regulation model for tissue differentiation during fracture healing: analysis of gap size and loading*, J. Biomech., 2002, 35, 1163–1171.

[21] BONNET A.S., DUBOIS G., LIPINSKI P., SCHOUMAN T., *submitted, In vivo study of human mandibular distraction osteogenesis. Part I: Bone transport force determination*, Acta Bioeng. Biomech., 2012, 14, 3–14.

[22] LABBÉ D., NICOLAS J., KALUZINSKI E., SOUBEYRAND E., SABIN P., COMPÈRE J.F., BÉNATEAU H., *Gunshot Wounds: Reconstruction of the lower face by osteogenic distraction*, Plast. Reconstr. Surg., 2005, 116, 1596–1603.

[23] LAUTERBURG M.T., EXNER G.U., JACOB H.A., *Forces involved in lower limb lengthening: an in vivo biomechanical study*, J. Orthop. Res., 2006, 24, 1815–1822.

[24] REINA-ROMO E., GÓMEZ-BENITO M.J., GARCÍA-AZNAR J.M., DOMÍNGUEZ J., DOBLARÉ M., *Growth mixture model of distraction osteogenesis: effect of pre-traction stresses*, Biomech. Model Mechanobiol., 2010, 9, 103–115.